Contributions of Mixed-Phase Clouds to Reduced Arctic Amplification

Ivy Tan[1,2], Trude Storelvmo[3], Mark Zelinka[4], Lazaros Oreopoulos[1], Dongmin Lee[1,5]
[1]NASA GSFC, [2]USRA, [3]Yale University, [4]Lawrence Livermore National Laboratory, [5]Morgan State University

Contact Information:
NASA GSFC
Code 613, 8800 Greenbelt Rd.
Building 33, Rm. B320, 20771, MD, USA

Phone: +1 (301) 614 6190
Email: `ivy.tan@nasa.gov`

Abstract

Earth's Arctic is particularly sensitive to global warming. The climate record shows that Arctic changes in surface temperatures far exceed that of the global mean, a phenomenon referred to as *Arctic amplification*. Here, we show that warming of the Arctic atmosphere causes mixed-phase clouds in the region to contain less ice and more supercooled liquid, which in turn tends to increase their amount and thickness, thereby inducing a positive feedback mainly by increasing downward longwave (LW) radiation at the surface. The increased downward LW radiation decreases the positive lapse rate feedback in the Arctic, thus resulting in reduced Arctic amplification. The strength of this feedback depends on the initial mean-state supercooled liquid fraction (SLF) and the ice crystal effective radii. We also show that reduced precipitation rates can result from large mean-state ice effective radii being replaced by relatively more smaller liquid droplets in the cloud phase feedback, despite having high mean-state SLFs, demonstrating the importance of the representation of cloud microphysics in the Arctic.

Method

- We ran a series of five simulations with increasing mean-state supercooled liquid fraction (SLF), where $SLF = \frac{liquid}{liquid+ice}$
- The five simulations, in increasing order of mean-state SLF are: Low-SLF, Control, CALIOP-SLF1, CALIOP-SLF2, High-SLF (Table 1)
- CALIOP-SLF1 and CALIOP-SLF2 were constrained to better match the SLF obtained from NASA's CALIOP Vertical Feature Mask from Nov. 1, 2007 to Dec. 31, 2013
- SLFs were computed on isotherms, using NCEP-DOE Reanalysis II data [1]
- Quasi-Monte Carlo (QMC) sampling of a 6-D cloud microphysical parameter space was used to constrain CALIOP-SLF1 and CALIOP-SLF2 (Table 2)
- Each simulation was run with both present-day and doubled CO_2 concentrations, at 1.9° × 2.5° resolution with NCAR's fully-coupled CAM5/CESM model, until the top of the atmosphere radiation balance $< 0.3\,\mathrm{Wm^{-2}}$

Table 1: Summary of Simulations

Name of Simulation	Description
Low-SLF	IN increased by a factor of 75
Control	Out-of-the-box CESM
CALIOP-SLF1*†	Satellite-constrained
CALIOP-SLF2*†	Satellite-constrained
High-SLF*	IN-free

*Includes modified detrainment scheme [2]
†Includes DeMott *et al.* [2015] [3] ice nucleation scheme in place of that of Meyers *et al.* [1992]

Table 2: Details pertaining to CALIOP-constrained simulations.

Panel A: Parameters in QMC-sampled Simulations

Process Investigated	Parameter	Default	Range
Ice nucleation	fin	1	[0,1]
WBF timescale for ice	10^{epsi}	0	[-6, 0]
WBF timescale for snow	10^{epss}	0	[-6, 0]
Ice crystal fall speed (s^{-1})	ai	700	[350,1400]
Stratiform cloud scavenging	sol_facti	1	[0.5,1]
Convective cloud scavenging	sol_factic	0.4	[0.2,0.8]

Panel B: Parameter Values in CALIOP-Constrained Simulations

Simulation	fin	$epsi(s)$	sol_facti	sol_factic	ai	Score‡
CALIOP-SLF1	0.49	−1.62	0.96	0.72	354	314
CALIOP-SLF2	0.19	−0.096	0.99	0.97	371	276

‡Score to determine “best” match to CALIOP observations defined as $\sum_{j=1}^{n}\sum_{i=1}^{m} e\ SCFM_{i,j}\ SCFO_{i,j}$ s, where $SCFM$ and $SCFMO$ are the modelled and observed SCFs, respectively, and i and j are the gridbox indices.

Results

Equilibrium climate sensitivity (ECS) increases with SLF (Figure 1a, b). This is due to the cloud phase feedback (Figure 2), which weakens with increasing SLF. However, the arctic amplification (AA) factor (Figure 1f) decreases in the opposite direction, and instead follows the weighted ice fraction (IF) (Figure 1c). This phenomenon can be explained by the mechanism shown in Figure 3.

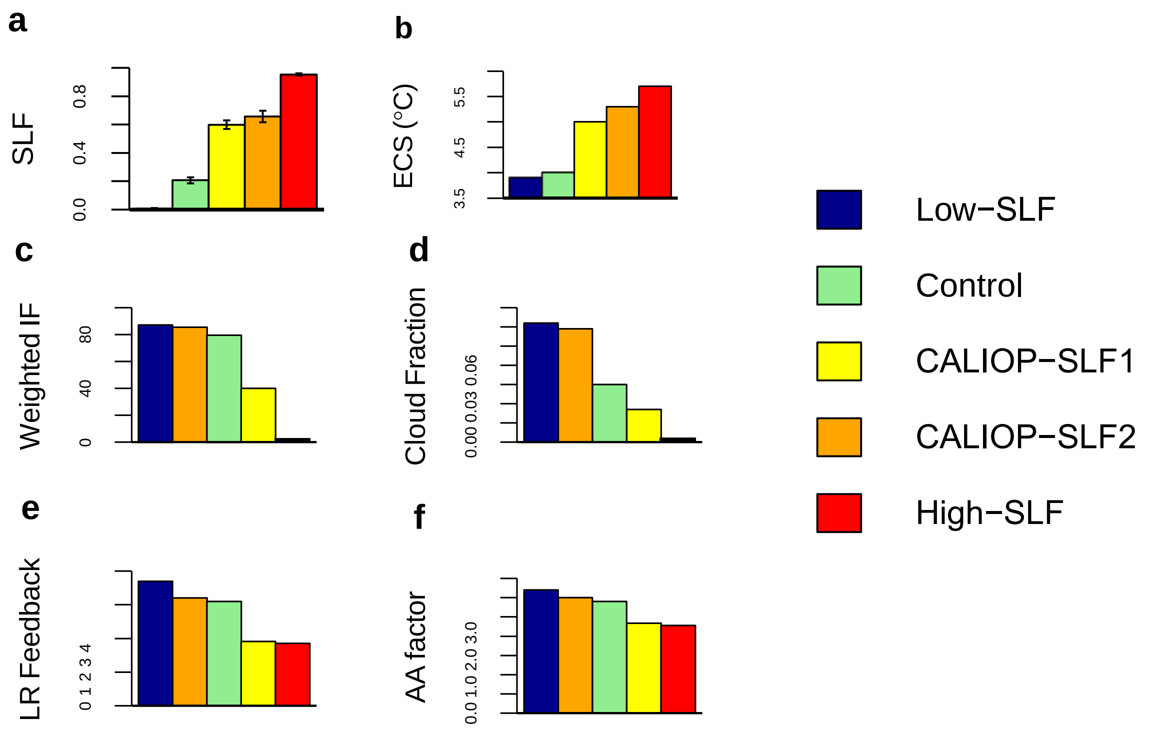

Figure 1: The link between SLF of mixed-phase clouds and ECS. (a) Mean-state extratropical SLFs at the −10°C. (b) ECS estimates in response to CO_2 doubling. (c) Weighted ice fraction (IF), equal to SLF weighted by the average effective radius in the Arctic lower troposphere. (d) Average Arctic cloud fraction (e) Average Arctic lapse rate feedback. (f) Arctic amplification (AA) factor, equal to the average Arctic surface temperature normalized by ECS.

Cloud Phase Feedback

The strength of the cloud phase feedback decreases with increasing SLF. Ice has been replaced with liquid throughout all mixed-phase cloud temperatures after CO_2 doubling in Low-SLF, but only at ∼−40°C in High-SLF (Figure 2). The increased (decreased) LWP in Low-SLF (High-SLF) after CO_2 doubling implies more (less) SW reflection and hence greater cooling (warming).

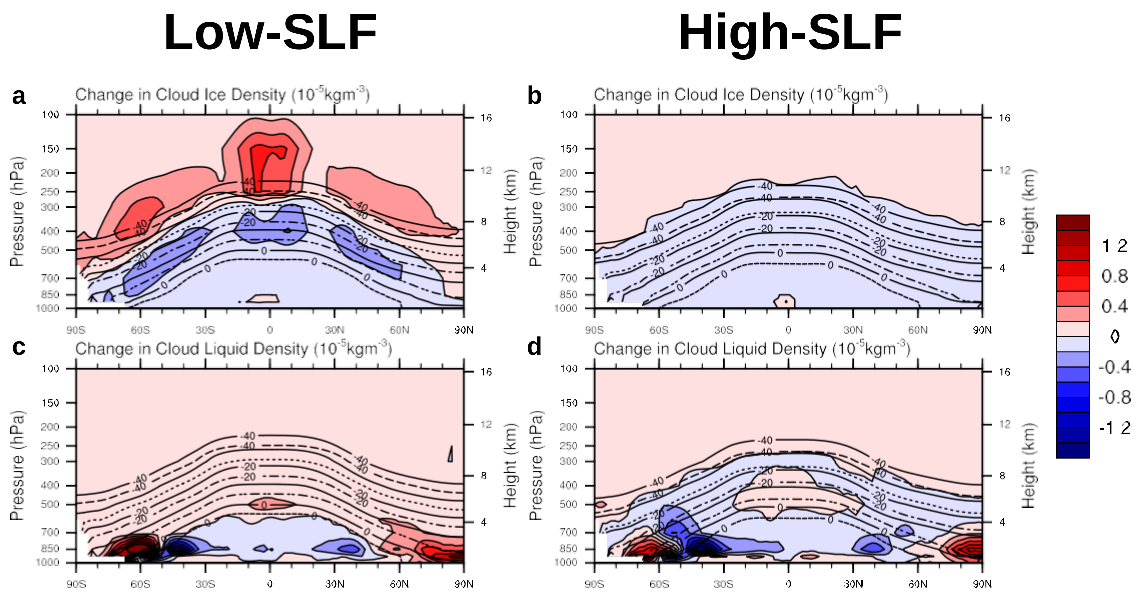

Figure 2: Weakening of the cloud-phase feedback. Pressure-latitude cross-sections of zonal mean-state changes in gridbox-averaged (a and b) cloud ice and (c and d) cloud liquid densities in [(a) and (c)] High-SLF and [(b) and (d)] Low-SLF in response to CO_2 doubling. Isotherms in the present-day (doubled) CO_2 simulations are displayed as dashed (solid) lines.

Mechanism of Reduced Arctic Amplification

A lower SLF implies that more liquid replaces ice after CO_2 doubling (cloud phase feedback). This causes cooling by increasing SW reflection at the top-of-the-atmosphere thereby resulting in a negative feedback to the warming induced by the initial CO_2 doubling (Figure 3, top feedback loop). However, more liquid replacing ice also extends the cloud lifetime (Figure 1d), which in turn increases LW at the surface, which increases the positive lapse rate feedback in the Arctic (Figure 1e). This increases AA. A higher mean-state SLF would therefore lead to reduced AA (Figure 1f).

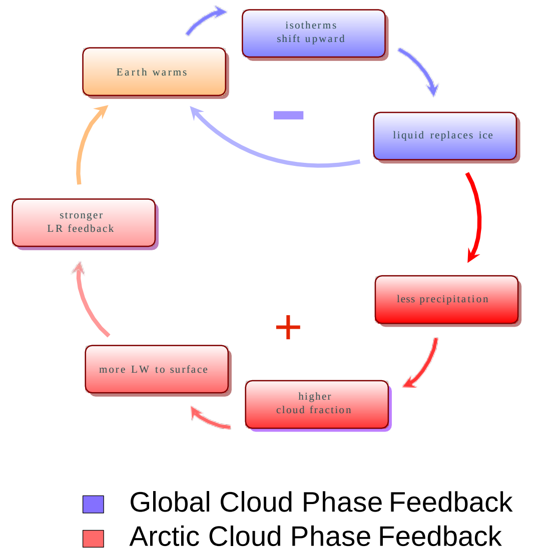
Earth warms
isotherms shift upward
liquid replaces ice
−
less precipitation
higher cloud fraction
more LW to surface
stronger LR feedback
+

🟦 Global Cloud Phase Feedback
🟥 Arctic Cloud Phase Feedback

Figure 3: Mechanism of reduced arctic amplification. The negative cloud phase feedback loop at the top applies globally; the positive feedback loop only occurs in the Arctic. A higher mean-state SLF decreases the strength of the negative feedback and also decreases the strength of the positive feedback that only occurs in the Arctic.

In the Arctic, the ice crystal effective radii in the lower troposphere in CALIOP-SLF2 are much larger than that of the other simulations (Figure 4). This causes CALIOP-SLF2 to behave more similarly to the lower SLF simulations (Low-SLF and Control), which we can account for by weighting SLF by the average ice crystal effective radius (Figure 1c). This demonstrates the importance of ice microphysics.

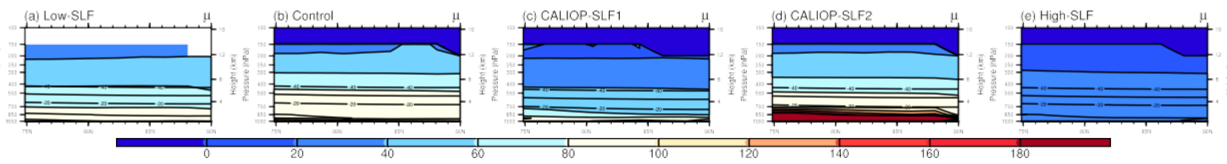

Figure 4: Mean-state ice crystal effective radius (in microns) for the five simulations.

Conclusions

- An underestimate of SLF leads to a simultaneous underestimate in ECS (due to a strengthened negative cloud phase feedback) and overestimate in AA (ultimately due to a strengthened positive Arctic lapse rate feedback).
- A mean state with relatively high SLF can behave as one with lower SLF by virtue of the fact that its ice crystals are larger in effective radius. Thus, when considering SLF, it is important to also factor in effective radius.

References

1 I. Tan, T. Storelvmo, and Y.-S. Choi, A comparison of the ice nucleating efficiencies of clean dust, polluted dust, and smoke aerosols in mixed-phase clouds based on spaceborne lidar observations. *JGR*, 119(11):6653–6665, 2014, doi:10.1002/2013JD021333.
2 I. Tan, T. Storelvmo, Sensitivity study on the influence of cloud microphysical parameters on mixed-phase cloud thermodynamic phase partitioning in CAM5. *J. Atm. Sci.*, 73(2):709-728, 2016, doi:10.1175/JAS-D-15-0152.1.
3 P. J. Demott *et al.*, Integrating laboratory and field data to quantify the immersion freezing ice nucleation activity of mineral dust particles. *ACP*, 2015.
4 J. M. Gregory *et al.*, A new method for diagnosing radiative forcing and climate sensitivity. *GRL*, 31(3), 2004, doi:10.1029/2003GL018747.

Acknowledgments

This research was supported by an appointment to the NASA Postdoctoral Research Program at NASA GSFC, administered by USRA under contract with NASA. This work was supported by NASA Headquarters under the NASA Earth and Space Science Fellowship Program, grant NNX14AL07H. We also acknowledge high-performance computing support from Yellowstone provided by National Center for Atmospheric Research?s Computational and Information Systems Laboratory, sponsored by NSF under grant 1352417.